Minocycline inhibits cytochrome *c* release and delays progression of amyotrophic lateral sclerosis in mice

Shan Zhu*, Irina G. Stavrovskaya†, Martin Drozda*, Betty Y. S. Kim*, Victor Ona*, Mingwei Li*, Satinder Sarang‡, Allen S. Liu*, Dean M. Hartley§, Du Chu Wu‖, Steven Gullans‡, Robert J. Ferrante¶#, Serge Przedborski‖☆, Bruce S. Kristal† & Robert M. Friedlander***

* *Neuroapoptosis Laboratory, Department of Neurosurgery, Brigham & Women's Hospital, Harvard Medical School, Boston, Massachusetts 02115, USA*
† *Burke Medical Research Institute, White Plains, New York 10605, USA*
‡ *Department of Medicine, Brigham & Women's Hospital, Harvard Medical School, Boston, Massachusetts 02115, USA*
§ *Center for Neurologic Diseases, Brigham & Women's Hospital, Harvard Medical School, Boston, Massachusetts 02115, USA*
‖ *Department of Neurology,* ☆ *Department of Pathology, Columbia University, New York, New York 10032, USA*
¶ *Geriatric Research Education and Clinical Center, Bedford VA Medical Center, Bedford, Massachusetts 01730, USA*
# *Neurology, Pathology, and Psychiatry Departments, Boston University School of Medicine, Boston, Massachusetts 02118, USA*
** *Departments of Biochemistry and Neuroscience, Weill Medical College of Cornell University, New York, New York 10021, USA*

Minocycline mediates neuroprotection in experimental models of neurodegeneration. It inhibits the activity[1–6] of caspase-1, caspase-3, inducible form of nitric oxide synthetase (iNOS) and p38 mitogen-activated protein kinase (MAPK). Although minocycline does not directly inhibit these enzymes, the effects may result from interference with upstream mechanisms resulting in their secondary activation. Because the above-mentioned factors are important in amyotrophic lateral sclerosis (ALS), we tested minocycline in mice with ALS[7–9]. Here we report that minocycline delays disease onset and extends survival in ALS mice. Given the broad efficacy of minocycline, understanding its mechanisms of action is of great importance. We find that minocycline inhibits mitochondrial permeability-transition-mediated cytochrome *c* release. Minocycline-mediated inhibition of cytochrome *c* release is demonstrated *in vivo*, in cells, and in isolated mitochondria. Understanding the mechanism of action of minocycline will assist in the development and testing of more powerful and effective analogues. Because of the safety record of minocycline, and its ability to penetrate the blood–brain barrier, this drug may be a novel therapy for ALS[10].

Minocycline is a second-generation tetracycline that effectively crosses the blood–brain barrier[10]. It has remarkable neuroprotective qualities in models of cerebral ischaemia, traumatic brain injury, and Huntington's and Parkinson's disease[1–3,5,6]. Members of the caspase cell death family, in particular caspase-1 and caspase-3, are activated and have important roles in these diseases[1,2,7,11]. In addition to caspases, iNOS is also upregulated and activated in these diseases[1,2,8]. Minocycline-mediated neuroprotection is associated with inhibition of caspase-1, caspase-3 and iNOS transcriptional upregulation and activation[1–3,5,6]. Inhibition of p38 MAPK and microglial activation have been associated with minocycline-mediated neuroprotection[1,4]. Despite all these neuroprotective properties of minocycline, its precise primary target is not known. The goals of the present study are to evaluate the effectiveness of minocycline on a mouse model of ALS, and investigate its mechanism of neuroprotection.

ALS is a chronic neurodegenerative disease characterized by progressive motor weakness resulting from selective motor neuron cell death[12]. Mortality is seen on the average four years following onset. The only proven therapy in humans, Riluzole, extends survival in humans by approximately three months[12]. It is therefore critical to identify new therapeutic strategies for ALS. Mutations in superoxide dismutase-1 (SOD1) have been linked to about 20% of patients with familial ALS[13]. Familial and sporadic forms of the disease have indistinguishable clinical and histopathological features. Transgenic mice expressing several of the mutant *SOD1* genes found in humans with ALS develop motor neuron symptoms and histopathology resembling features of the human disease[14,15]. Caspase-1 and caspase-3 are activated in neurons of ALS mice[9]. As caspases have an important role in ALS, and minocycline interferes with caspase pathways, we evaluated its effect on one of the ALS mouse models expressing the mutant human $SOD1^{G93A}$ transgene. Minocycline (10 mg per kg body weight per day) was injected beginning at five weeks of age. Mutant $hSOD1^{G93A}$ transgenic mice were evaluated weekly on a Rotarod to follow disease progression. Onset of impaired motor performance in minocycline-treated mice was delayed to 109.0 ± 1.5 days of age as compared to 90.3 ± 2.2 days in saline-treated mice ($P < 0.001$) (Fig. 1a–c). Minocycline administration extended survival from 125.6 ± 3.4 days to 136.8 ± 1.2 days ($P < 0.01$) (Fig. 1b, d). Minocycline-mediated neuroprotection in $hSOD1^{G93A}$ mice was independently confirmed (by S.P.) using a slightly modified protocol. In this trial, minocycline administration started at six weeks of age at a slightly higher dose (11 mg per kg body weight per day). Mortality of saline-treated mice was 126.3 ± 2.7 days as compared to 139.0 ± 2.1 days of the minocycline-treated mice ($n = 8$ per group, $P < 0.05$). These results demonstrate effectiveness of minocycline in this transgenic ALS model.

We then investigated the mechanism of minocycline-mediated neuroprotection. The known activities of minocycline include inhibition of caspase-1 and caspase-3 transcriptional upregulation and activation. However, minocycline does not directly inhibit caspase-1 or casapse-3 activity[2]. A challenge in elucidating the primary neuroprotective target of minocycline *in vivo*, especially in chronic neurodegenerative diseases, is that many pathways become activated during the progression of the disease as a result of a secondary reactive process. To determine the primary target (or targets) of minocycline, we searched for *in vitro* models where cell death is inhibited by minocycline. As minocycline mediates remarkable neuroprotection in ischaemia and traumatic brain injury[1,3], we evaluated its effect on *N*-methyl-D-aspartate (NMDA)-mediated cell death in primary cerebrocortical neurons. Minocycline inhibited NMDA-induced cell death (Fig. 2a). In addition, minocycline inhibited death of SH-SY5Y neuroblastoma cells treated with either H_2O_2 or thapsigargin (THG) (Fig. 2b, c). Similar to its broad *in vivo* neuroprotective properties, minocycline inhibits cell death in a variety of *in vitro* models of cell death, suggesting that minocycline inhibits a critical shared step in the execution of the death program. As minocycline does not directly inhibit caspase-1 or caspase-3, we evaluated its effect on caspase-9 activation and cytochrome *c* release[2]. Minocycline-mediated inhibition of THG-induced cell death correlates with inhibition of caspase-9 and of caspase-3 activation as well as of cytochrome *c* release (Fig. 2d, e).

Cytochrome *c* release from the mitochondria into the cytoplasm is a potent physiological stimulus for caspase-9 and caspase-3 activation[16]. Therefore, inhibition of cytochrome *c* release might be a primary target of minocycline. To directly probe this question, we evaluated the effect of minocycline on release of cytochrome *c* from cell-free mitochondrial preparations. Minocycline inhibited both calcium- and Bid-induced cytochrome *c* release in purified mouse liver mitochondria (Fig. 3a)[17,18]. Owing to the critical role of mitochondria in apoptotic pathways, the relation between minocycline and inhibition of cytochrome *c* release is probably an important clue as to one of its primary/direct mechanisms of action[16].

To confirm that mitochondria are direct targets of minocycline in the brain, and further probe into its mechanism of action, we evaluated the effect of minocycline on isolated non-synaptosomal

brain mitochondria. Cytochrome *c* release, changes in mitochondrial membrane potential ($\Delta\Psi$), Ca^{2+} transport, oxygen consumption and transmittance at 660 nm were monitored following Ca^{2+} addition (Fig. 3c–e and data not shown). As demonstrated in isolated liver mitochondria, and in the above-described models, minocycline inhibited cytochrome *c* release in isolated brain mitochondria. Minocycline addition was associated with alteration in several mitochondrial parameters, such as a decrease in $\Delta\Psi$ (Fig. 3d), but the change in transmittance (Fig. 3e) was the only change whose dose-specific effect reflected that of inhibition of cytochrome *c* release. Specifically, minocycline prevented most of the increase in transmittance that begins immediately on Ca^{2+} addition. These studies, conducted in concentrated mitochondrial solutions appropriate for biochemical studies, required 200 μM minocycline for complete protection (Fig. 3a–e). But expressing minocycline levels as concentrations overstates requirements if minocycline is accumulated or acts stoichiometrically, in which case minocycline levels are more appropriately expressed in mol per

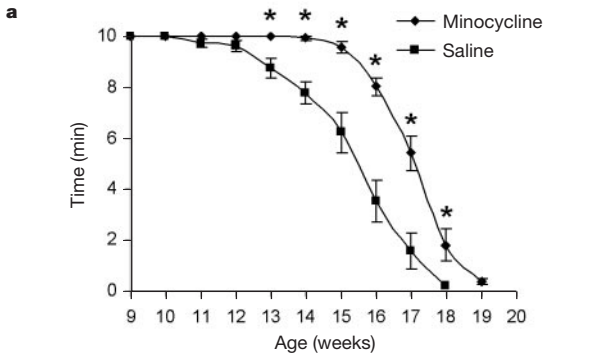

b

	Saline (*n*=10)	Minocycline (*n*=10)	*P* value
Onset	90.3±2.2	109±1.5	<0.001
Mortality	125.6±3.4	136.8±1.2	<0.01

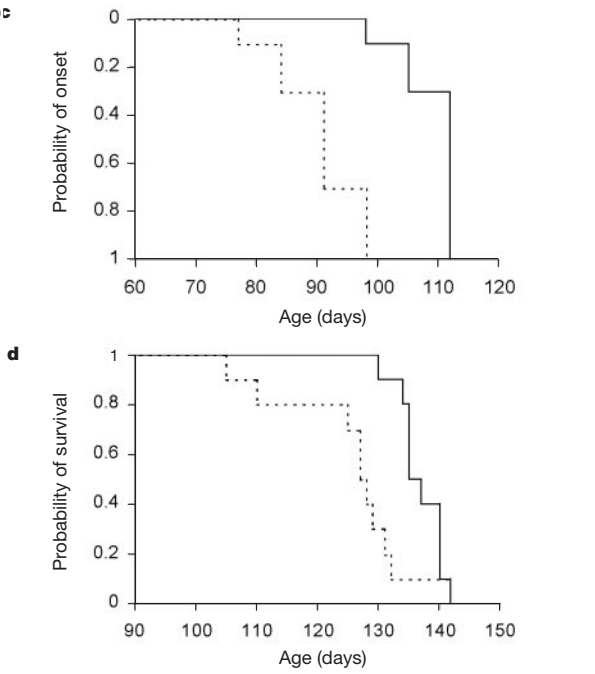

Figure 1 Minocycline delays onset and extends survival in ALS mice. **a**, Rotarod evaluation (see Methods) of *hSOD1* ^{G93A} transgenic ALS mice treated with saline or minocycline ($n = 10$ per group; asterisk, $^*P < 0.05$; error bars represent s.e.m.). **b**, Onset of motor deficits and mortality of ALS mice treated with minocycline or saline. **c**, **d**, Cumulative probability of onset of Rotarod deficits (**c**) and survival (**d**) in *hSOD1* ^{G93A} mice. Onset of Rotarod deficit and mortality were significantly delayed in ALS mice treated with minocycline compared to mice treated with saline. Solid line, minocycline-treated ALS mice; dashed line, saline-treated control ALS mice.

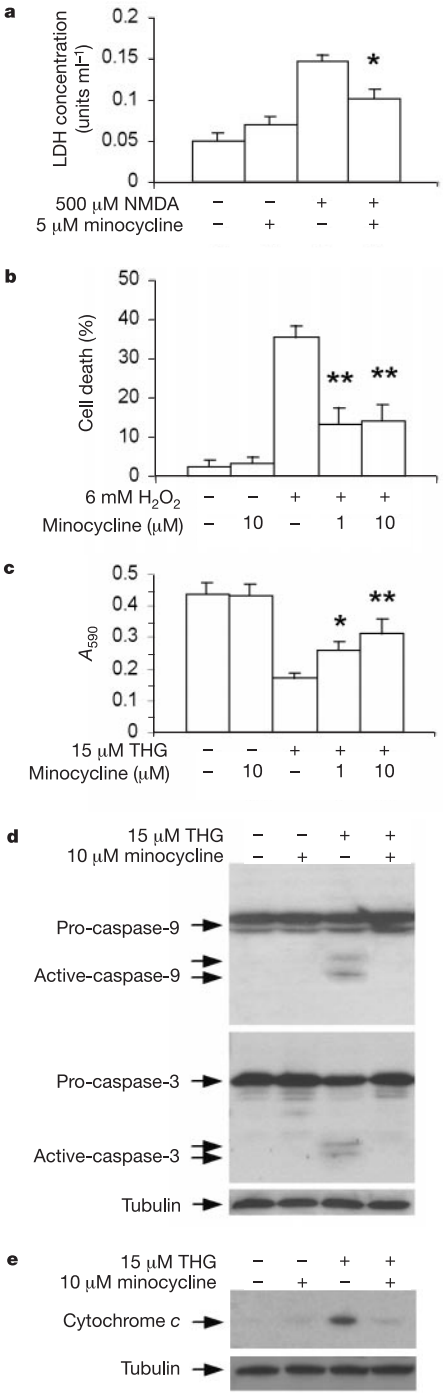

Figure 2 Minocycline inhibits cell death, caspase activation and cytochrome *c* release. **a**, Rat primary cortical neurons exposed to *N*-methyl-D-aspartate (NMDA) in the presence or absence of minocycline. **b**, **c**, H_2O_2-mediated (**b**) and thapsigargin (THG)-mediated (**c**) SH-SY5Y cell death and its inhibition by minocycline. **d**, Caspase-9 and caspase-3 western blots of lysates of SH-SY5Y cells exposed to THG. **e**, Cytochrome *c* western blots of cytosolic fraction of SH-SY5Y cells exposed to THG. In cell death assays, data are representative of three independent experiments. (asterisk, $P < 0.05$; double asterisk, $P < 0.01$; error bars represent s.e.m.) A_{590}, absorbance at 590 nm.

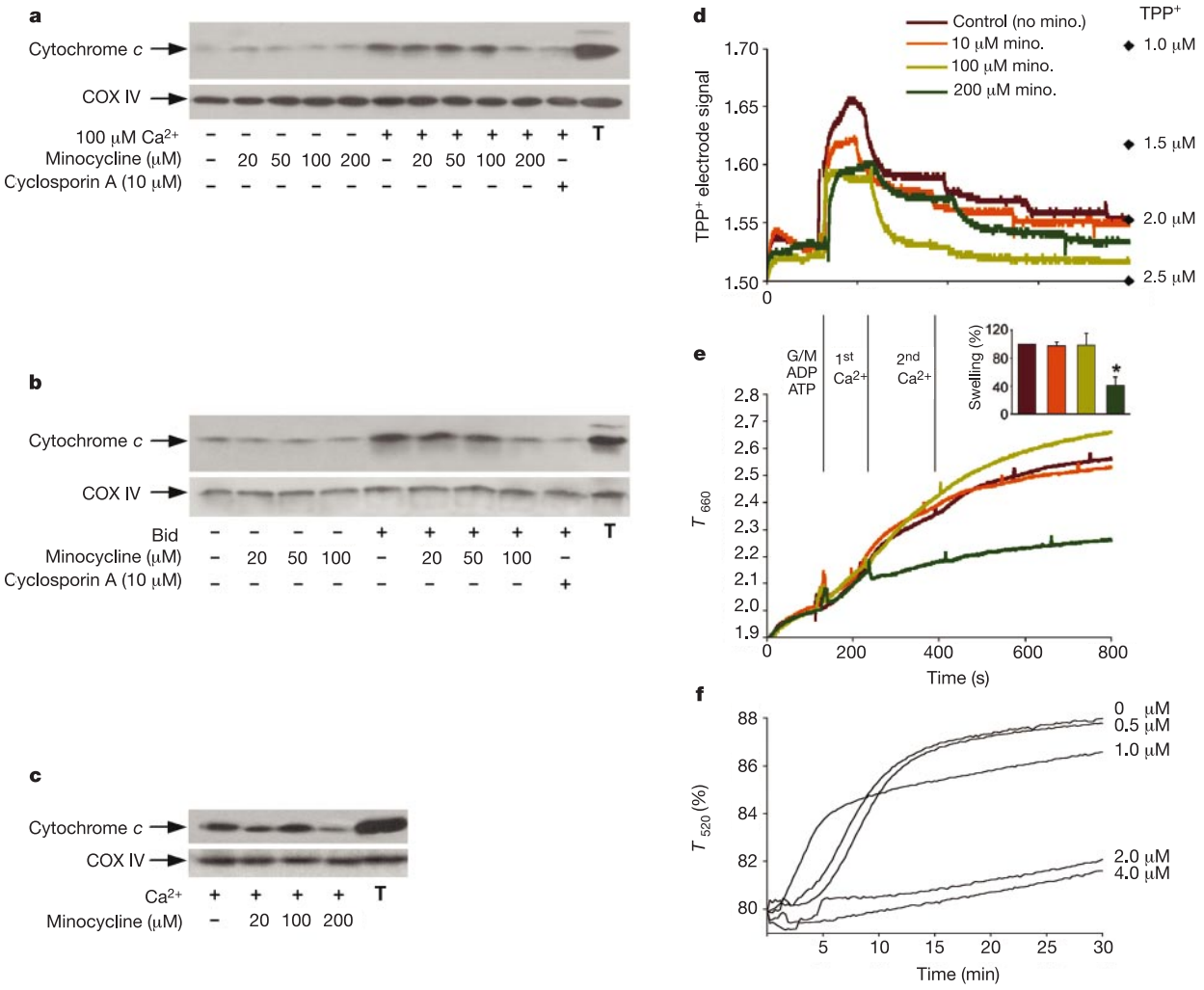

Figure 3 Minocycline inhibits cytochrome *c* release and swelling in purified mitochondria. **a**,**b**, Mouse liver mitochondria (0.5 mg ml^{-1}) were incubated with minocycline or cyclosporin A and cytochrome *c* release was induced by $CaCl_2$ (**a**) or purified Bid protein (**b**). T, total mitochondrial cytochrome *c*. COX IV was used as a loading control. **c**–**e**, Cytochrome *c* release (**c**) $\Delta\Psi$ (**d**) and light transmittance (**e**) in rat non-synaptosomal brain mitochondria (1 mg ml^{-1}) exposed to 40 μM Ca^{2+} pulses in the presence of varying minocycline concentrations. Inset in **e**, mean ± s.d. of the swelling (increase in transmittance) relative to control at 600 s (shown as 100%). Bars coloured as main key. Asterisk, $P < 0.01$ versus 0, 10 and 100 μM minocycline, ANOVA followed by the statistically conservative Tukey/Kramer *post hoc*. **f**, Representative traces of effects of minocycline on swelling under conditions associated with PT induction in diluted rat liver mitochondria (0.03 mg ml^{-1}). Initial transmittance (T%) normalized to start at a common point (mean adjustment <1% of initial value).

mg protein. Co-titration of minocycline and mitochondria demonstrated minocycline-mediated inhibition of mitochondrial swelling at physiologically relevant concentrations of 2–4 μM in isolated rat liver mitochondria (≥40 nmol per mg protein, Fig. 3f, and data not shown). Traces are representative of a total of 24 experiments (3 independent mitochondrial preparations, 2 mitochondrial concentrations (0.1 mg ml^{-1}, 0.03 mg ml^{-1}), 2 substrates (glutamate/malate, succinate), 2 duplicates) on minocycline-mediated protection. For 0.1 mg per ml protein, 12 out of 12 samples were protected by 4 μM minocycline (40 nmol per mg protein); for 0.03 mg per ml protein, 12 out of 12 samples were protected by 2 μM minocycline (66 nmol per mg protein). The described minocycline-mediated effects were highly reproducible and statistically significant ($P < 0.0001$ analysis of variance, ANOVA, followed by the Fisher protected least significant difference (PLSD) *post hoc* test).

To confirm the findings of minocycline-mediated inhibition of cytochrome *c* release *in vivo*, we evaluated whether minocycline-mediated neuroprotection in ALS mice is associated with inhibition of cytochrome *c* release. Consistent with a previous report, release of cytochrome *c* in spinal cords of ALS mice correlates with disease progression[15]. Minocycline treatment significantly inhibited release of cytochrome *c* in ALS mice ($n = 5$, $P < 0.05$) (Fig. 4a, b). As a confirmatory marker of efficacy, we show that minocycline inhibits caspase-3 activation in spinal cords of ALS mice (Fig. 4c). To extend these findings, we demonstrate that minocycline inhibits cerebral ischaemia-mediated cytochrome *c* release ($n = 5$, $P < 0.01$) (Fig. 4d, e). These results provide *in vivo* confirmation and support to the finding of minocycline-mediated inhibition of cytochrome *c* release in cells and in isolated mitochondria.

The data obtained are most consistent with a model in which minocycline acts directly on the mitochondria to alter PT-mediated cytochrome *c* release. Although other possibilities cannot be ruled out, several lines of evidence point to involvement of PT in the effects demonstrated by minocycline. Release of cytochrome *c* from isolated liver mitochondria occurs following exposure to exogenous Ca^{2+}, the standard PT challenge, or Bid, which has been shown to accelerate PT induction, and is prevented in both cases by cyclosporin, the standard PT inhibitor[19,20]. In non-synaptosomal mitochondria, minocycline failed to significantly block Ca^{2+}-cycling driven loss of $\Delta\Psi$ (Fig. 3d and data not shown), but did consistently

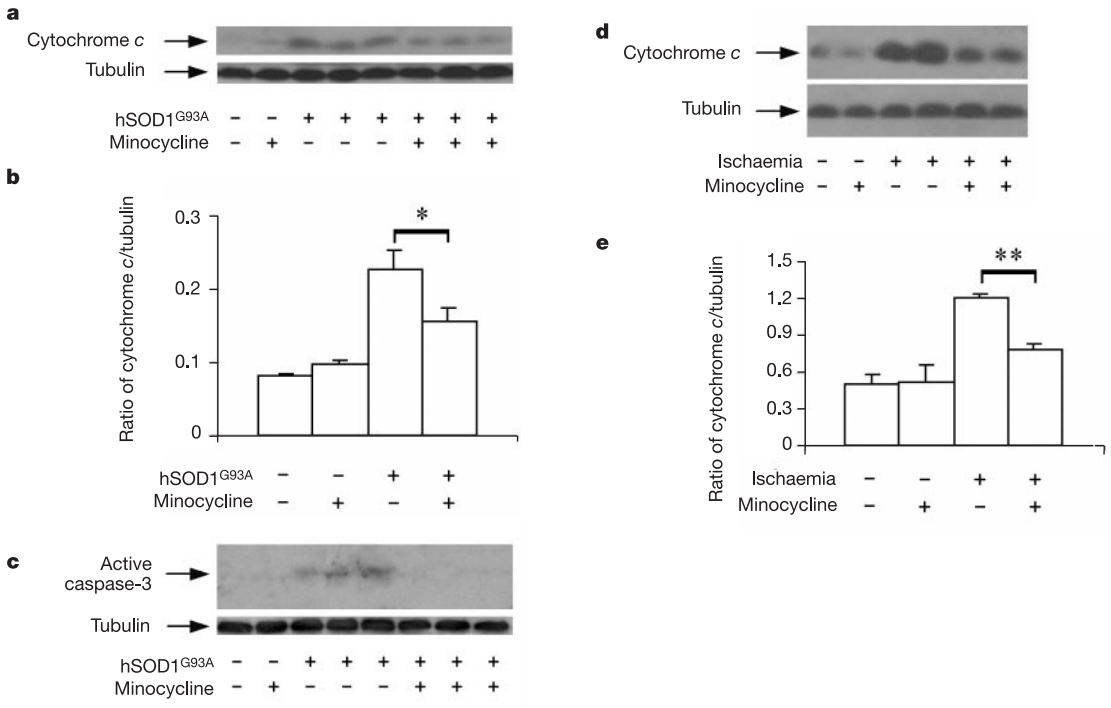

Figure 4 Minocycline inhibits cytochrome *c* release in ALS and ischaemia. **a**,**b**, ALS mice were injected with minocycline for 10 days starting at eight weeks of age. Spinal cord cytosolic components were evaluated by western blot for cytochrome *c* release (**a**). Densitometric quantification of cytochrome *c* release ($n = 5$, asterisk, $P < 0.05$) (**b**). **c**, Caspase-3 western blot of spinal cord lysate of ALS mice treated with/without minocycline using an antibody specific for activated caspase-3 (p17). **d**, Cytosolic components of the ischaemic territory of mouse brains were fractionated and analysed for cytochrome *c* release. **e**, Densitometric quantification of cytochrome *c* release ($n = 5$, double asterisk, $P < 0.01$).

prevent over 50% of the total change in transmittance (Fig. 3e). Transmittance is the physical equivalent of the absorbance change considered a standard hallmark of PT induction in liver mitochondria and more controversially, one measure of 'PT-like' behaviour in non-synaptosomal preparations[21,22]. Given that the exact mechanism mediating cytochrome *c* release remains unclear and controversial, these results do not rule out the possibility that alternative PT-independent pathways might exist, resulting in cytochrome *c* release[16,20,23].

We have validated the mechanism of action of minocycline at three levels: using cell-free mitochondrial preparations, using cell based death models, and *in vivo* using ALS mice and cerebral ischaemia models. As release of cytochrome *c* is a shared feature of many neurological disorders, inhibition of PT-mediated cytochrome *c* release by minocycline explains, at least in part, the broad inhibition of cell death (both *in vivo* and *in vitro*) mediated by this drug. Minocycline is, to our knowledge, the first non-toxic drug with a proven human safety record shown to inhibit cytochrome *c* release. Compounds such as minocycline will probably provide important synergism with compounds targeting other pathological mechanisms of disease progression[2,9,24]. As demonstrated in this study, minocycline delays disease progression in a mouse model of ALS. Given its safety in chronic diseases, its oral bioavailability and its ability to cross the blood–brain barrier, minocycline could be evaluated for its effectiveness in human ALS[10]. Minocycline is at present being evaluated in human trials for Huntington's disease. Understanding the mechanism of action of minocycline will assist in the development and testing of more powerful and effective analogues. □

Methods

Minocycline treatment of ALS mice

ALS mice (Jackson Laboratories) were injected intraperitoneally daily with saline or minocycline (Sigma). Strength and coordination were evaluated weekly by Rotarod (Columbus Instruments). Disease onset was defined as the first day a mouse could not remain on the Rotarod for 10 min at 15 r.p.m. Mortality was scored as age of death or age when the mouse was unable to right itself within 30 s (ref. 9).

NMDA neurotoxicity

Primary cortical neurons isolated from E16 rats and cultured as described[25]. After two weeks, cultures were exposed for six hours to 500 μM NMDA (Sigma) with or without a two-hour minocycline preincubation. Cytotoxicity was assayed by measuring lactate dehydrogenase (LDH) release[25].

Minocycline inhibition of SH-SY5Y cell death

Human neuroblastoma SH-SY5Y cells were preincubated with media containing minocycline for 24 h at 37 °C, and later exposed to 6 mM H_2O_2 for 4 h at 37 °C. Cells were then incubated with calcein-AM (1 μM, Molecular Probes) in PBS for 40 min at 37 °C. Cell viability was determined using an LJL 96, 384 Analyst (Molecular Devices) fluorescence reader. Viability is converted to cell death ratio (Fig. 2b). For THG experiments, cells were preincubated with minocycline for 1 h and then exposed to 15 μM THG (Sigma). After 12 h, cell death was evaluated by MTT assay (Roche).

Middle cerebral artery occlusion

C57/B6 mice (18–20 g) were injected with minocycline at 45 mg per kg body weight 4 h before ischaemia, then at 22.5 mg per kg body weight twice a day[1]. After 120 min of middle cerebral artery occlusion, blood flow was restored[26]. Brains were removed after 24 h and the ischaemic territory dissected for evaluation of cytochrome *c* release.

Tissue and cell cytosolic fractionation

Brains or spinal cord samples were homogenized (10 mM HEPES, pH 7.4, 250 mM sucrose, 10 mM KCl, 1.5 mM $MgCl_2$, 1 mM EDTA, 1 mM EGTA, 1 mM dithiothreitol (DTT), 50 μM *N*-benzoxycarbonyl-Val-Ala-Asp-fluoromethylketone (zVAD-fmk)) plus protease inhibitor cocktail (Roche) in a Kontes dounce homogenizer with a B pestle (Kontes Glass Co.). Cytosolic component was fractionated as described[24]. SH-SY5Y cell cytosolic fraction was prepared 6 h after THG treatment using the same protocol as for mouse brains.

Western blot

For caspase activation, samples were lysed in RIPA buffer with protease inhibitors. For cytochrome *c* release, cytosolic component from tissue (40 μg) or cells (10 μg) was loaded for evaluation. Cytochrome *c*, caspase-9 and caspase-3 antibodies were purchased from PharMingen; COX IV antibody from Clontech.

Liver and brain mitochondria preparation

Mouse liver mitochondria were prepared as described and resuspended in MRM buffer (250 mM sucrose, 10 mM HEPES, pH 7.5, 1 mM ATP, 5 mM sodium succinate, 80 μM ADP, 2 mM K_2HPO_4) at a concentration of 0.5 mg ml^{-1} (ref. 18). Rat liver mitochondria were isolated from 4–6-month-old Fischer 344 × brown Norway F_1 rats by differential centrifugation as described, except the final wash and resuspension buffer had no EGTA, EDTA or BSA[27]. Non-synaptosomal rat brain mitochondria were prepared from forebrains of ~8-week Fischer 344 × brown Norway rats (Ficoll gradient purification)[28,29].

In vitro cytochrome *c* release

An aliquot of 25 μl of 0.5 mg ml^{-1} mouse liver mitochondrial preparation was preincubated with minocycline or cyclosporin A for 5 min in MRM buffer. Mitochondria were incubated with 100 μM $CaCl_2$ or 100 ng of purified mouse Bid protein[17] at 30 °C for 30 min ($CaCl_2$) or for one hour (Bid). Mixtures were centrifuged at 10,000*g* at 4 °C for 10 min and the supernatant evaluated by western blot.

ΔΨ/swelling measurements

Rat brain mitochondria (1 mg ml^{-1} in 100 mM KCl, 75 mM mannitol, 25 mM sucrose, 10 mM Tris, 1 mM K-PO_4 (pH 7.3)) containing tetraphenyl phosphonium (TPP^+), 25 μM Ca^{2+} (from buffer and TPP^+ stock) and minocycline (see key in Fig. 3d, e) were added at $t = 0$ and energized where marked (Fig. 3d, e) with 5 mM glutamate, 5 mM malate, 1 mM ATP and 80 μM ADP. Bolus doses of 40 μM Ca^{2+} were added where shown (Fig. 3d, e). Simultaneous measurement of ΔΨ and light transmittance in stirred samples was accomplished using a four-channel respiration system designed by B. Krasnikov (ref. 30, and manuscript in preparation). Oxygen uptake, ΔΨ, and Ca^{2+} were measured using Clark, TPP^+, and Ca^{2+}-sensitive electrodes, respectively. A_{660} was measured using a diode. Experiments were carried out in triplicate. Plots shown are representative. Mixtures were sampled and centrifuged at 10,000*g* at 4 °C for 10 min. Supernatants were evaluated for cytochrome *c* (Fig. 3c).

Rat liver mitochondria were used for minocycline-mitochondria co-titration. PT induction was assessed spectrophotometrically by suspending mitochondria at 25 °C in 200 μl of 310 mM sucrose, 30 mM KCl, 3 mM K-HEPES (pH 7.3), with 5 μM added Ca^{2+}. Samples with 0.1 mg mitochondria per ml had 100 μM K-PO_4; samples with 0.03 mg mitochondria per ml had 30 μM K-PO_4. Changes in transmittance at 520 nm were followed for 30 min using a SpectraMax 250 Plate Reader (Molecular Dynamics). Minocycline does not display appreciable absorbance at this wavelength.

Light scattering data are qualitatively identical at the two wavelengths used. The lower wavelength (520 nm) was used on the plate reader because it gives a slightly better signal:noise profile. The higher wavelength (660 nm) was used in the four-channel system because the light-emitting diode can only be used at that wavelength.

Received 21 February; accepted 5 April 2002.

1. Yrjanheikki, J., Keinanen, R., Pellikka, M., Hokfelt, T. & Koistinaho, J. Tetracyclines inhibit microglial activation and are neuroprotective in global brain ischemia. *Proc. Natl Acad. Sci. USA* **95,** 15769–15774 (1998).
2. Chen, M. *et al.* Minocycline inhibits caspase-1 and caspase-3 expression and delays mortality in a transgenic mouse model of Huntington disease. *Nature Med.* **6,** 797–801 (2000).
3. Sanchez Mejia, R. O., Ona, V. O., Li, M. & Friedlander, R. M. Minocycline reduces traumatic brain injury-mediated caspase-1 activation, tissue damage, and neurological dysfunction. *Neurosurgery* **48,** 1393–1401 (2001).
4. Tikka, T., Fiebich, B. L., Goldsteins, G., Keinanen, R. & Koistinaho, J. Minocycline, a tetracycline derivative, is neuroprotective against excitotoxicity by inhibiting activation and proliferation of microglia. *J. Neurosci.* **21,** 2580–2588 (2001).
5. Wu, D. C. *et al.* Blockade of microglial activation is neuroprotective in the 1-methyl-4-phenyl-1,2,3,6-tetrahydropyridine mouse model of Parkinson disease. *J. Neurosci.* **22,** 1763–1771 (2002).
6. Du, Y. *et al.* Minocycline prevents nigrostriatal dopaminergic neurodegeneration in the MPTP model of Parkinson's disease. *Proc. Natl Acad. Sci. USA* **98,** 14669–14674 (2001).
7. Friedlander, R. M., Brown, R. H., Gagliardini, V., Wang, J. & Yuan, J. Inhibition of ICE slows ALS in mice. *Nature* **388,** 31 (1997).
8. Almer, G., Vukosavic, S., Romero, N. & Przedborski, S. Inducible nitric oxide synthase up-regulation in a transgenic mouse model of familial amyotrophic lateral sclerosis. *J. Neurochem.* **72,** 2415–2425 (1999).
9. Li, M. *et al.* Functional role of caspase-1 and caspase-3 in an ALS transgenic mouse model. *Science* **288,** 335–339 (2000).
10. Brogden, R. N., Speight, T. M. & Avery, G. S. Minocycline: A review of its antibacterial and pharmacokinetic properties and therapeutic use. *Drugs* **9,** 251–291 (1975).
11. Ona, V. O. *et al.* Inhibition of caspase-1 slows disease progression in a mouse model of Huntington's disease. *Nature* **399,** 263–267 (1999).
12. Rowland, L. P. & Shneider, N. A. Amyotrophic lateral sclerosis. *N. Engl. J. Med.* **344,** 1688–1700 (2001).
13. Rosen, D. R. *et al.* Mutations in Cu/Zn superoxide dismutase gene are associated with familial amyotrophic lateral sclerosis. *Nature* **362,** 59–62 (1993).
14. Gurney, M. E. *et al.* Motor neuron degeneration in mice that express a human Cu,Zn superoxide dismutase mutation. *Science* **264,** 1772–1775 (1994).
15. Wong, P. C. *et al.* An adverse property of a familial ALS-linked SOD1 mutation causes motor neuron disease characterized by vacuolar degeneration of mitochondria. *Neuron* **14,** 1105–1116 (1995).
16. Green, D. R. & Reed, J. C. Mitochondria and apoptosis. *Science* **281,** 1309–1312 (1998).
17. Li, H., Zhu, H., Xu, C. J. & Yuan, J. Cleavage of BID by caspase 8 mediates the mitochondrial damage in the Fas pathway of apoptosis. *Cell* **94,** 491–501 (1998).
18. Luo, X., Budihardjo, I., Zou, H., Slaughter, C. & Wang, X. Bid, a Bcl2 interacting protein, mediates cytochrome c release from mitochondria in response to activation of cell surface death receptors. *Cell* **94,** 481–490 (1998).
19. Zamzami, N. *et al.* Bid acts on the permeability transition pore complex to induce apoptosis. *Oncogene* **19,** 6342–6350 (2000).
20. Bernardi, P., Scorrano, L., Colonna, R., Petronilli, V. & Di Lisa, F. Mitochondria and cell death. Mechanistic aspects and methodological issues. *Eur. J. Biochem.* **264,** 687–701 (1999).
21. Kristal, B. S. & Dubinsky, J. M. Mitochondrial permeability transition in the central nervous system: induction by calcium cycling-dependent and -independent pathways. *J. Neurochem.* **69,** 524–538 (1997).
22. Friberg, H., Connern, C., Halestrap, A. P. & Wieloch, T. Differences in the activation of the mitochondrial permeability transition among brain regions in the rat correlate with selective vulnerability. *J. Neurochem.* **72,** 2488–2497 (1999).
23. Shimizu, S., Narita, M. & Tsujimoto, Y. Bcl-2 family proteins regulate the release of apoptogenic cytochrome c by the mitochondrial channel VDAC. *Nature* **399,** 483–487 (1999).
24. Guegan, C., Vila, M., Rosoklija, G., Hays, A. P. & Przedborski, S. Recruitment of the mitochondrial-dependent apoptotic pathway in amyotrophic lateral sclerosis. *J. Neurosci.* **21,** 6569–6576 (2001).
25. Hartley, D. M. *et al.* Protofibrillar intermediates of amyloid beta-protein induce acute electrophysiological changes and progressive neurotoxicity in cortical neurons. *J. Neurosci.* **19,** 8876–8884 (1999).
26. Friedlander, R. M. *et al.* Expression of a dominant negative mutant of interleukin-1 beta converting enzyme in transgenic mice prevents neuronal cell death induced by trophic factor withdrawal and ischemic brain injury. *J. Exp. Med.* **185,** 933–940 (1997).
27. Kristal, B. S. & Brown, A. M. Apoptogenic ganglioside GD3 directly induces the mitochondrial permeability transition. *J. Biol. Chem.* **274,** 23169–23175 (1999).
28. Lai, J. C. & Clark, J. B. Preparation of synaptic and nonsynaptic mitochondria from mammalian brain. *Methods Enzymol.* **55,** 51–60 (1979).
29. Kristal, B. S., Staats, P. N. & Shestopalov, A. I. Biochemical characterization of the mitochondrial permeability transition in isolated forebrain mitochondria. *Dev. Neurosci.* **22,** 376–383 (2000).
30. Krasnikov, B. F., Kuzminova, A. E. & Zorov, D. B. The Ca^{2+}-induced pore opening in mitochondria energized by succinate-ferricyanide electron transport. *FEBS Lett.* **419,** 137–140 (1997).

Acknowledgements

We thank E. Friedlander for editorial assistance, B. Krasnikov for discussion concerning the 4-channel mitochondrial chamber, and M. Lukyanova for technical assistance. Mouse Bid expression construct was provided by H. Li and J. Yuan. This work was supported by Project A.L.S. (R.M.F., S.G., S.P.), the NIH (R.M.F., D.M.H, R.J.F., S.P., B.S.K.), the Huntington's Disease Society of America (R.M.F.), the Hereditary Disease Foundation (R.M.F., B.S.K.), the Muscular Dystrophy Association (R.M.F., S.P.), the Veterans Administration (R.J.F.), Hope for ALS (S.G.), Ride for ALS (S.G.), ALS Association (S.P.), the US Department of Defense (S.P.), the Lowenstein Foundation (S.P.), the Smart Foundation (S.P.), and the Parkinson's Disease Foundation (S.P.).

Competing interests statement

The authors declare that they have no competing financial interests.

Correspondence and requests for materials should be addressed to R.M.F. (e-mail: rfriedlander@rics.bwh.harvard.edu).

Extensive and divergent circadian gene expression in liver and heart

Kai-Florian Storch*, Ovidiu Lipan†, Igor Leykin†, N. Viswanathan‡, Fred C. Davis‡, Wing H. Wong†§ & Charles J. Weitz*

** Department of Neurobiology, Harvard Medical School; † Department of Biostatistics, Harvard School of Public Health; and ‡ Department of Biology, Northeastern University, Boston, Massachusetts 02115, USA*
§ Department of Statistics, Harvard University, Cambridge, Massachusetts 02138, USA

Many mammalian peripheral tissues have circadian clocks[1–4]; endogenous oscillators that generate transcriptional rhythms thought to be important for the daily timing of physiological processes[5,6]. The extent of circadian gene regulation in peripheral tissues is unclear, and to what degree circadian regulation in different tissues involves common or specialized pathways is unknown. Here we report a comparative analysis of circadian gene expression *in vivo* in mouse liver and heart using oligonucleotide arrays representing 12,488 genes. We find that peripheral circadian gene regulation is extensive (≥8–10% of the genes expressed in each tissue), that the distributions of circadian phases in the two tissues are markedly different, and that very